Supplemental Figure I

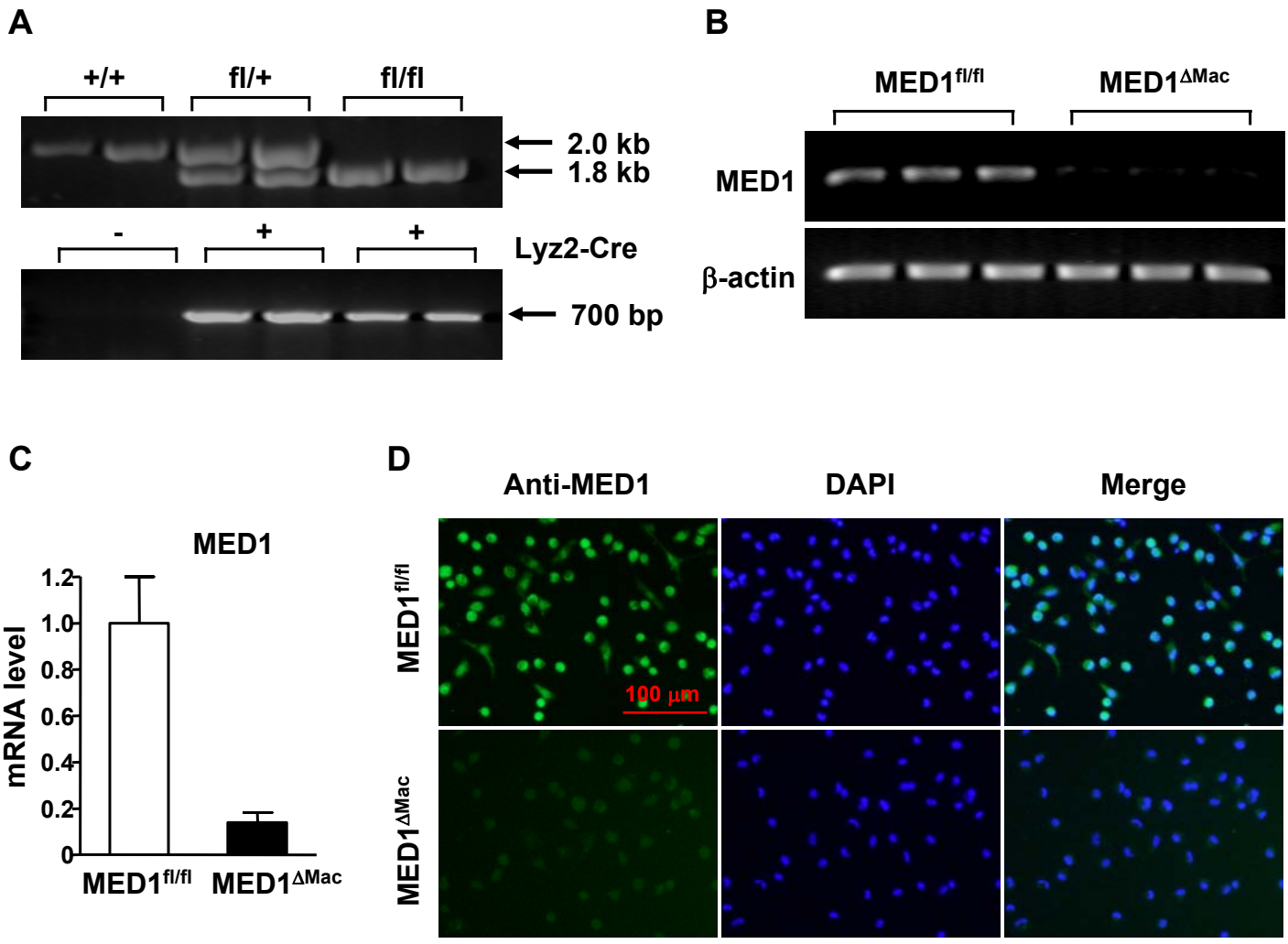

Supplemental Figure I. Macrophage-specific MED1 knockout. (A) PCR genotyping of mice carrying MED1 (top) and Cre (bottom). (B,C) PMs were isolated from MED$^{fl/fl}$ and MED1$^{\Delta Mac}$ mice (n=6 for each group) and used for detection of MED1 expression by semi-quantitative PCR (B) and qPCR (C). (D) PMs from MED$^{fl/fl}$ and MED1$^{\Delta Mac}$ mice were examined by immunofluorescence staining with the use of anti-MED1 or DAPI. The merged images reveal the presence of MED1 in the nuclei of the wild-type MED$^{fl/fl}$ mice.

Supplemental Figure II

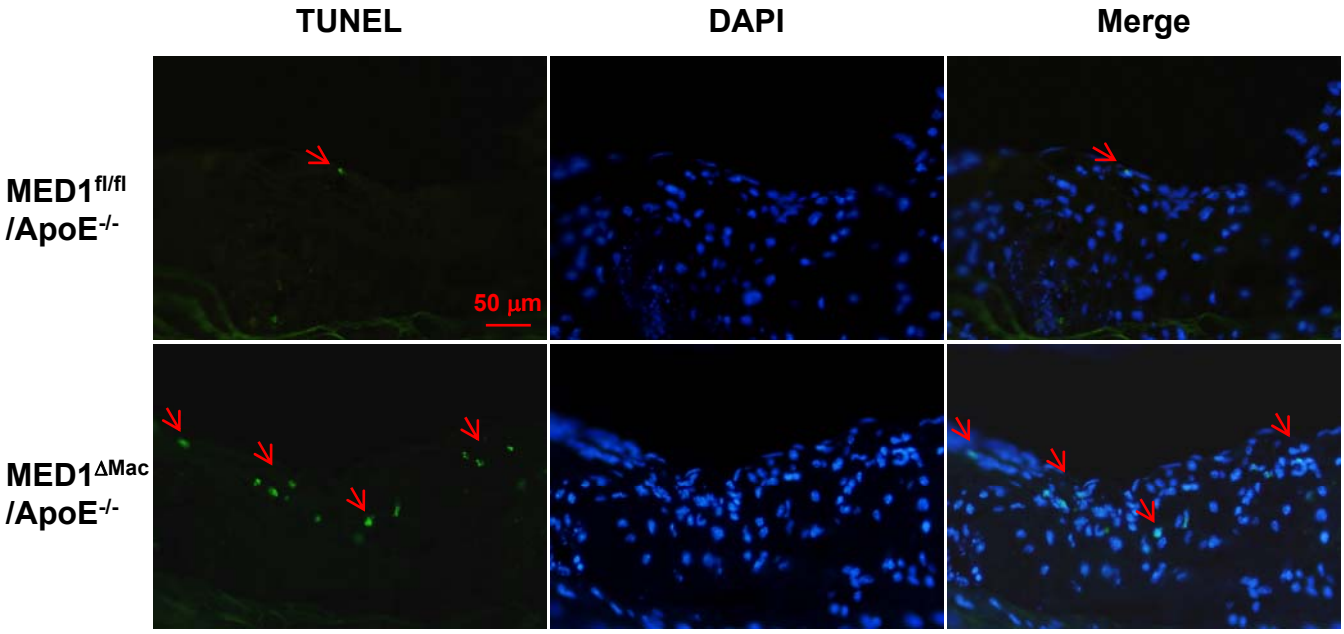

Supplemental Figure II. Increased apoptosis of aortic root in MED1$^{\Delta Mac}$/ApoE$^{-/-}$ mice. MED1$^{fl/fl}$/ApoE$^{-/-}$ and MED1$^{\Delta Mac}$/ApoE$^{-/-}$ mice were fed on Western diet for 12 weeks. Apoptotic changes of aortic roots were assessed by TUNEL staining. Merge indicates DAPI and TUNEL overlap. Red arrows indicate TUNEL positive cells. The graph are representative of 6 mice per genotype with similar results.

Supplemental Figure III

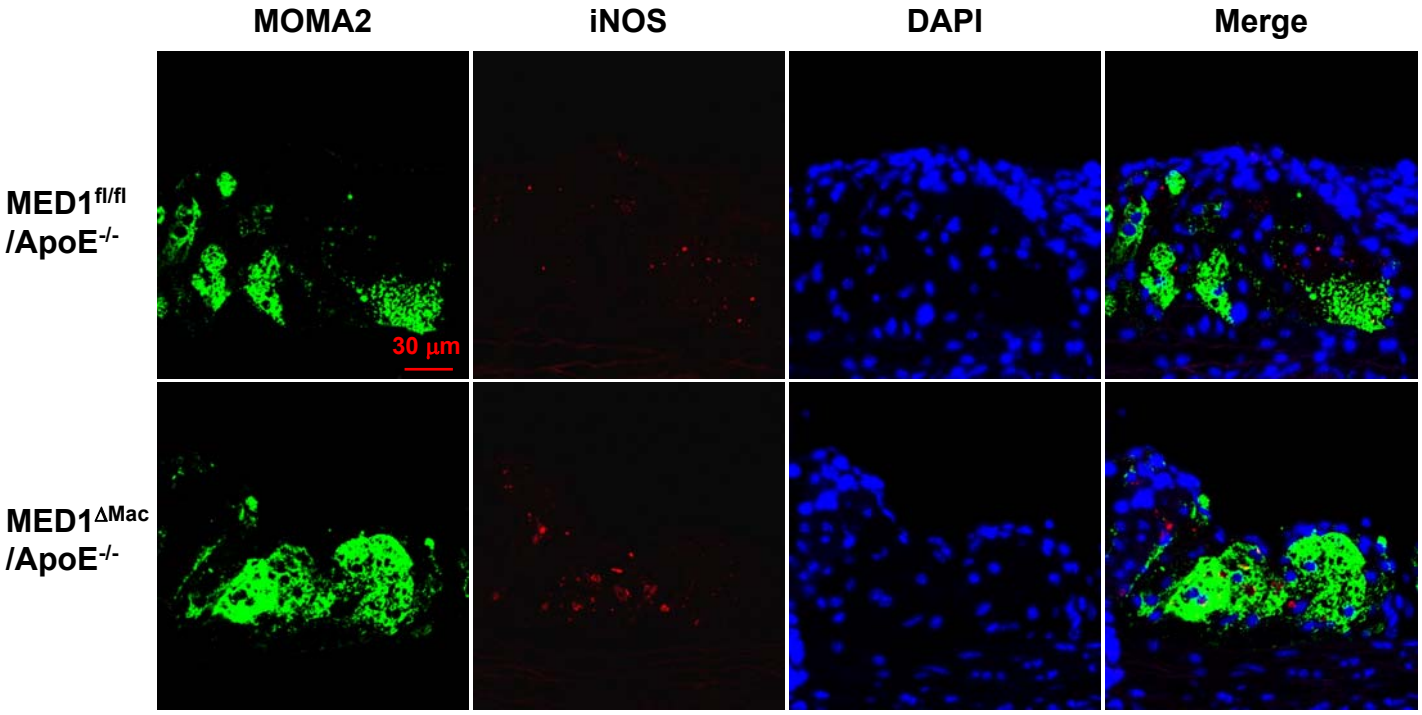

Supplemental Figure III. M1-like macrophages were increased in the early stage of atherosclerosis in MED1$^{\Delta Mac}$/ApoE$^{-/-}$ mice. Immunostaining of atherosclerotic lesions from MED1$^{fl/fl}$/ApoE$^{-/-}$ and MED1$^{\Delta Mac}$/ApoE$^{-/-}$ mice fed on Western diet for 4 weeks. Macrophages were identified as MOMA2-positive (green) cells. M1-like macrophages were identified as iNOS-positive (red) cells. Merge indicates co-expression of MOMA2 and iNOS. The graph are representative of 5-6 mice per genotype with similar results.

Supplemental Figure IV

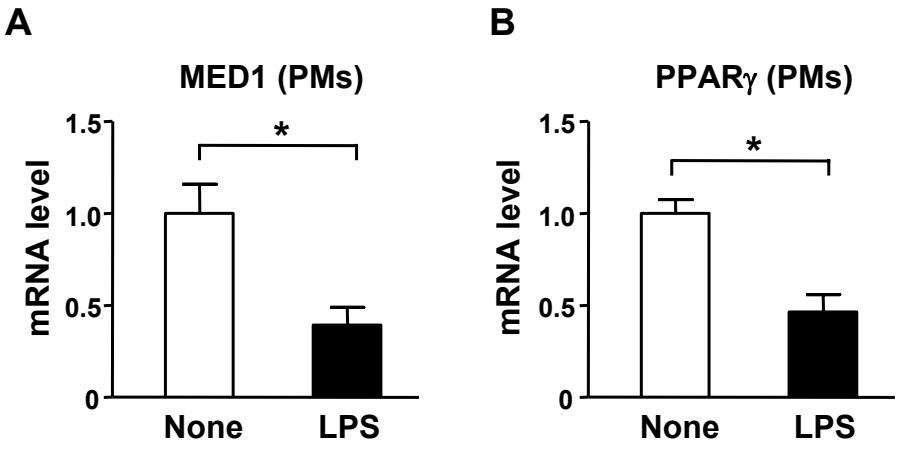

Supplemental Figure IV. MED1 and PPARγ expression is inhibited by M1 stimuli in PMs. MED1 (A) and PPARγ (B) mRNA level in $MED^{fl/fl}$ PMs after stimulation with LPS (50 ng/ml) for 6 hr. Graphs represent mean±SEM from 6 mice per group. * $p<0.05$.

Supplemental Figure V

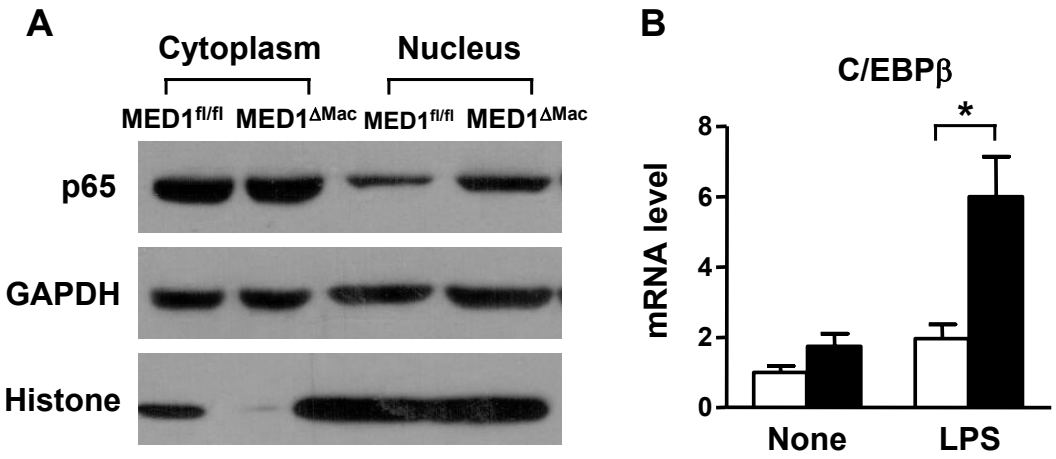

Supplemental Figure V. The increased expression of p65 and C/EBPβ in MED1-deficient macrophages. PMs were isolated from MED1$^{fl/fl}$ mice and MED1$^{\Delta Mac}$ littermates (n=12 in each group in A, n=6 in each group in B). (A) Western blot analysis of the nucleus and cytoplasm protein level of p65. GAPDH and histone bands were used as loading controls. (B) qPCR analysis of the C/EBPβ mRNA level in MED1$^{fl/fl}$ and MED1$^{\Delta Mac}$ PMs treated with or without LPS (50 ng/ml) for 6 hr. * p<0.05.

Supplemental Figure VI

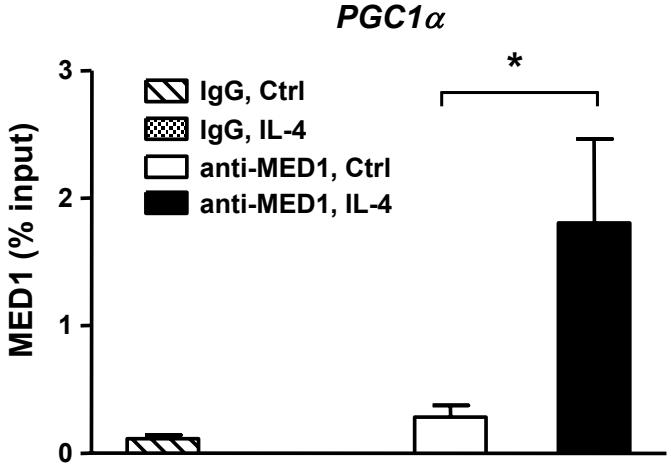

Supplemental Figure VI. A positive control of a known MED1 target gene PGC1α. RAW264.7 cells were treated with or without IL-4 (10 ng/ml) for 16 hr. ChIP assay was performed to detect the enrichment of MED1 at the promoter of *PGC1α*.

Supplemental Figure VII

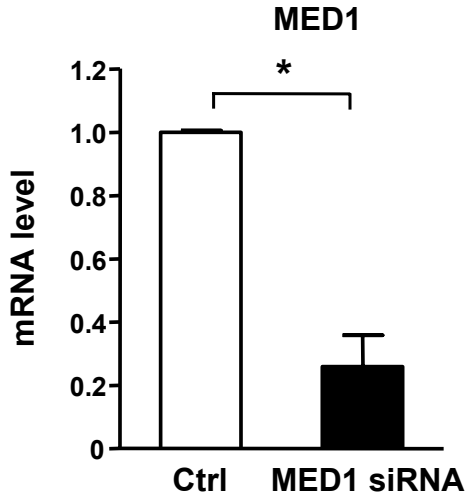

Supplemental Figure VII. Down-regulation of MED1 expression by MED1 siRNA in RAW264.7 cells. RAW264.7 cells were transfected with control siRNA or MED1 siRNA for 24 hr, and then MED1 mRNA expression was detected by qPCR. Data are mean±SEM from 3 independent experiments. * $p<0.01$.

Supplemental Figure VIII

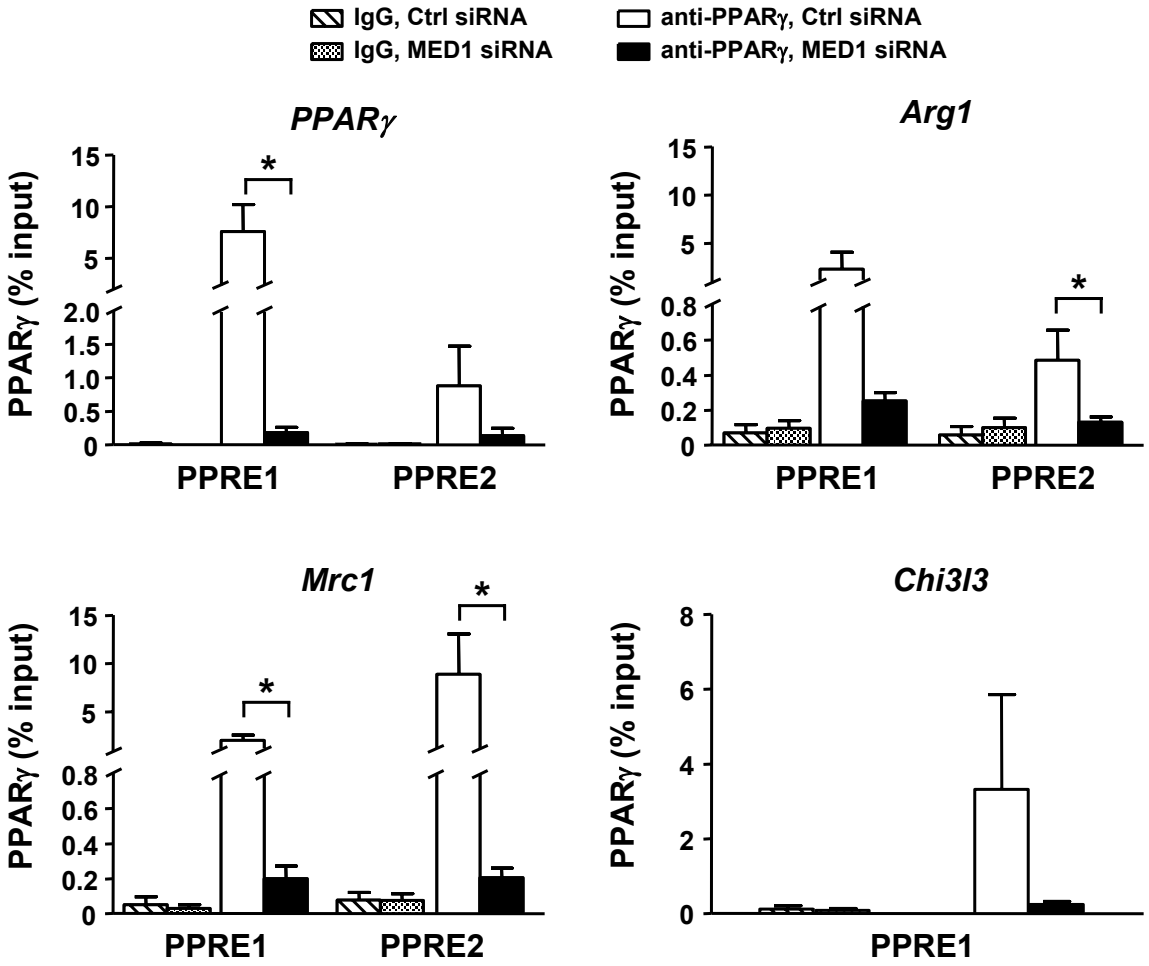

Supplemental Figure VIII. MED1 knockdown decreased the binding of PPARγ to the PPRE in the promoter region of M2 genes. RAW264.7 cells were transfected with control or MED1 siRNA for 24 hr, and then nuclear extracts were obtained. ChIP assay was performed to detect PPARγ enrichment at the upstream region of the *PPARγ*, *Arg1*, *Mrc1,* and *Chi3l3* gene. The primer sets used in qPCR were sequences adjacent to the predicted PPREs. IgG was used as the isotype control. Data represent as % of input and are mean±SEM from 3 independent experiments * $p<0.05$.

Supplemental Figure IX

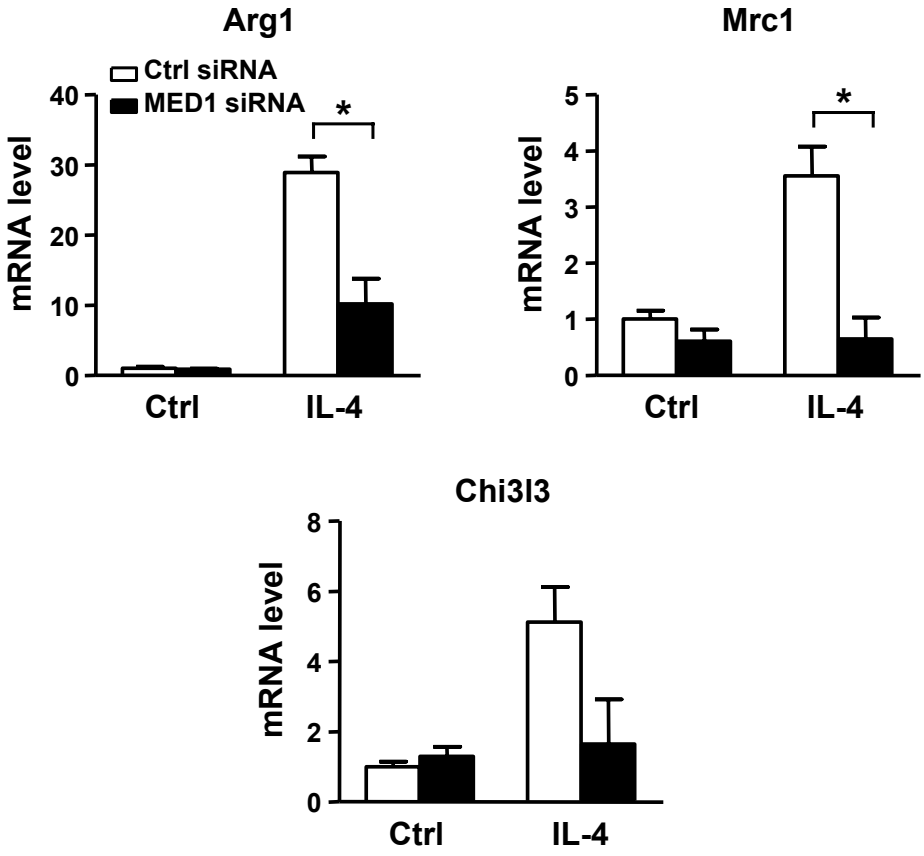

Supplemental Figure IX. MED1 is required for IL-4-induced M2 polarization. RAW264.7 cells were transfected with control siRNA or MED1 siRNA for 6 hr prior to treatment with or without IL-4 (10 ng/ml) for 16 hr. qPCR was performed to detect the mRNA level of Arg1, Mrc1, and Chi3l3. Data are mean±SEM from 3 independent experiments. * $p<0.05$.

Supplemental Figure X

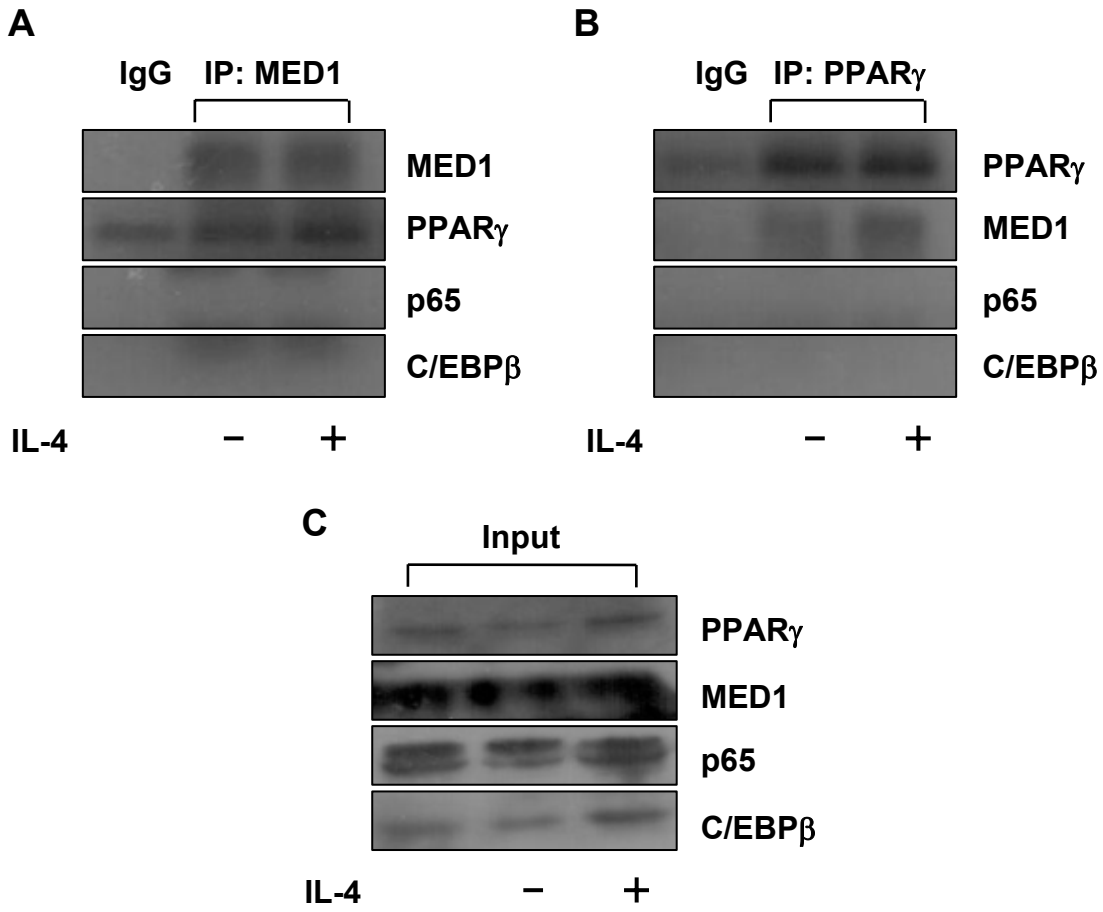

Supplemental Figure X. MED1 interacts with PPARγ rather than NF-κB and C/EBPβ under IL-4 treatment. RAW264.7 cells were treated with or without IL-4 (10 ng/ml) for 16 hr, MED1 (A) and PPARγ (B) was immunoprecipitated. In (C), cell lysates prior to IP were loaded as input controls. All samples were then immunoblotted with anti-MED1, anti-PPARγ, anti-p65, or anti-C/EBPβ antibody.

Supplemental Figure XI

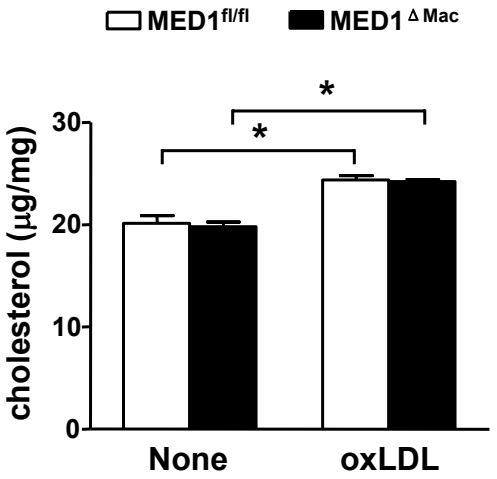

Supplemental Figure XI. MED1 deficiency does not affect cholesterol levels. MED1$^{fl/fl}$ and MED1$^{\Delta Mac}$ macrophages were incubated with or without oxLDL (50 μg/ml) for 24 hr. Cellular cholesterol contents were normalized to the milligram of cellular protein. Data are mean±SEM from triplicate determinations.

Supplemental Figure XII

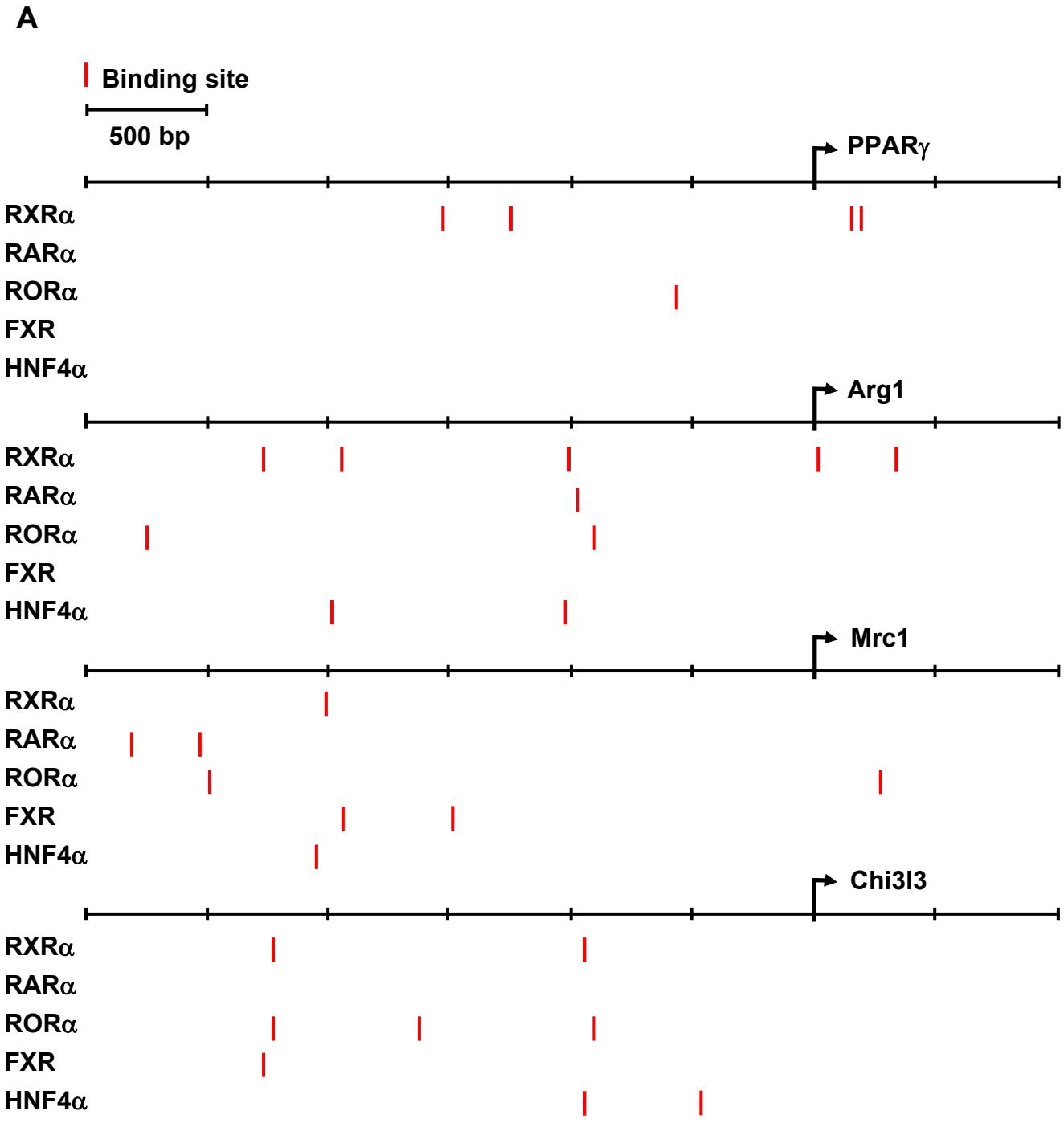

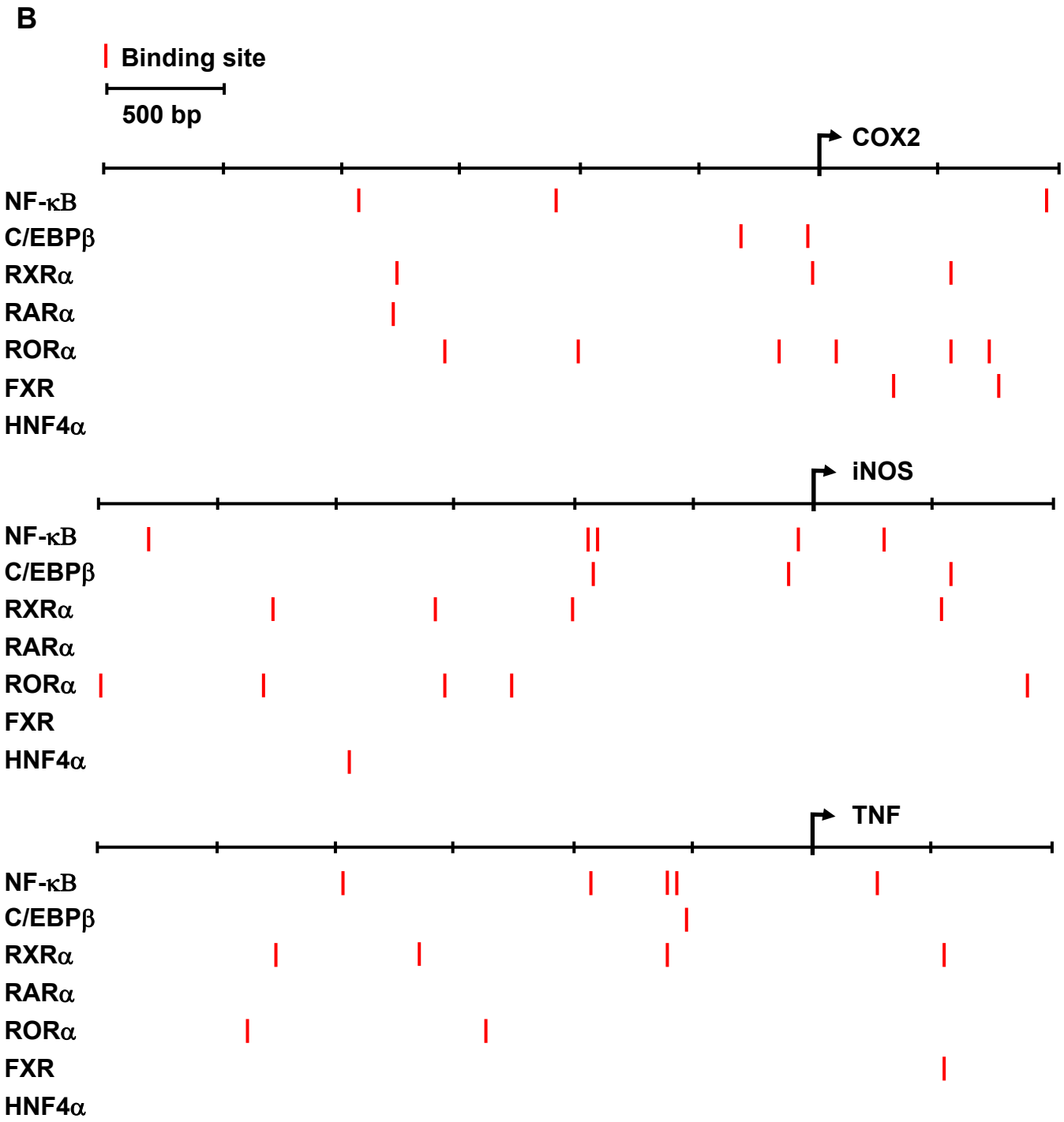

Supplemental Figure XII. The TF binding sites of other nuclear receptors in promoters of several M2 and M1 genes. Bioinformatics analysis of the TF binding sites of other nuclear receptors (RXRα, RARα, RORα, FXR, HNF4α, NF-κB and C/EBPβ) in the upstream region of M2 marker genes (*PPARγ*, *Arg1*, *Mrc1,* and *Chi3l3)* (A), *and* M1 marker genes (*COX2, iNOS* and *TNF*) (B) by JASPAR database. -3000 bp upstream to 1000 bp downstream of these genes were used for prediction. All these nuclear receptors interact with MED1 through which regulate target genes expression. Arrows mark the location of TSS and orientation of the genes, red line indicates the location of the binding sites of these transcription factors on target genes, and every scale means 500 bp.

Supplemental Table I. Total plasma cholesterol and triglycerides levels (mg/dL) in male MED1$^{fl/fl}$/ApoE$^{-/-}$ and MED1$^{\Delta Mac}$/ApoE$^{-/-}$ mice fed a chow diet

Group of mice	Plasma lipid	0 weeks	4 weeks	8 weeks	12 weeks
MED1$^{fl/fl}$/ApoE$^{-/-}$ (n=12)	TC	468±31	546±31	580±44	683±54
	TG	101±11	165±22	143±28	131±24
	LDL-C	309±26	373±34	328±30	490±38
	HDL-C	28±2	33±5	36±6	29±4
MED1$^{\Delta Mac}$/ApoE$^{-/-}$ (n=12)	TC	449±27	512±39	526±27	614±37
	TG	115±9	159±18	118±14	96±6
	LDL-C	292±17	309±30	293±19	412±33
	HDL-C	28±4	30±5	37±7	26±5

Supplemental Table II. Total plasma cholesterol and triglycerides levels (mg/dL) in male MED1$^{fl/fl}$/ApoE$^{-/-}$ and MED1$^{\Delta Mac}$/ApoE$^{-/-}$ mice after a Western diet for 12 weeks

Mice group	Plasma lipid	0 weeks	4 weeks	8 weeks	12 weeks
MED1$^{fl/fl}$/ApoE$^{-/-}$ (n=12)	TC	441±27	1122±70	1127±84	1319±99
	TG	206±29	278±26	266±30	314±40
	LDL-C	199±12	513±36	648±40	442±51
	HDL-C	58±10	78±18	80±11	81±25
MED1$^{\Delta Mac}$/ApoE$^{-/-}$ (n=15)	TC	408±18	1125±70	1326±62	1373±70
	TG	193±29	283±26	339±33	269±28
	LDL-C	183±9	567±42	774±50	550±62
	HDL-C	61±11	68±14	115±18	72±12

Supplemental Table III. Total plasma cholesterol and triglycerides levels (mg/dL) in male LDLR$^{-/-}$ mice transplanted with MED1$^{fl/fl}$ and MED1$^{\Delta Mac}$ bone marrow

Mice group	Plasma lipid	0 weeks	4 weeks	8 weeks	12 weeks
MED1$^{fl/fl}$ (n=7)	TC	244±11	629±26	546±50	905±29
	TG	110±8	111±9	159±19	345±30
	LDL-C	92±15	322±32	268±40	494±30
	HDL-C	79±7	101±4	114±3	109±9
MED1$^{\Delta Mac}$ (n=9)	TC	244±10	598±31	595±38	823±62
	TG	110±4	116±15	171±24	255±30
	LDL-C	112±9	311±20	293±31	456±44
	HDL-C	76±3	97±3	114±4	81±11